

Measurement of rotation and distortion of opaque surfaces by laser light scattering

Stefan Bosse, Wilfried Staude

July 14, 2000

Abstract

We present an experimental method to measure velocity gradients caused by distortions and rotations of arbitrary light scattering surfaces. The method is sensitive, gauge free and has a fairly high resolution. It is based on the scattering of a coherent plane light wave at the surface and the evaluation of the intensity pattern of the scattered light in the far field by use of a CCD-camera. By proper choosing the scattering geometry one can measure definite components of the velocity gradient of the surface.

1 Introduction

If a rough surface is illuminated with coherent light a characteristic random intensity pattern is observed on a screen placed in an arbitrary distance from the illuminated surface. This pattern is widely known as speckle pattern. Any changes of the scattering surface generally produce changes of the speckle pattern. This fact can be used to determine quantitatively changes of the scattering surface.

Different methods to measure surface distortions have been developed which are based on the analysis of the pattern changes. Most techniques are based on interferometry [1], holography [2], or speckle-photography [3]. They allow the simultaneous recording of large areas of the surface, surface changes are then determined from two successive recordings. By use of an electronic camera real time measurements are possible.

With the methods just mentioned, which are generally imaging methods, local displacements of a scattering surface are measured. Quantitative data on distortions or rotations must then be determined from these data by calculating the difference of displacements at different points on the surface. The advantage of these methods to give information on large areas of the surface changes is contrasted by the disadvantage that the accuracy of the obtained data is reduced by the very fact that three different measurement values must be combined in order to obtain one value for rotation/distortion: Two displacement values at different points and the distance of these points.

Hayashi and Kitagawa [4] were able to develop a rather simple technique to measure rotations of a cylinder with high accuracy. They recorded the motion of the speckle pattern with a video camera and could from these recordings resolve rotations about $6 \cdot 10^{-6}$ rad. This method, however, only works reliably if the rotation axis is known, and if no changes of the scattering surface other than this rotation occur.

Takai and Asakura [5] described a technique based on the evaluation of the cross-correlation function of two recorded speckle patterns, which allows a rather accurate determination of surface distortions. They give, however, no information on the accuracy of the measured displacement values.

More recently, Zhuang et al. [6] measured three-dimensional displacements with a holospeckle interferometry method. They resolve displacements in the sub-micrometer region. Again no information on the accuracy of these data is given which prevents a assessment of the accuracy of distortion data obtain with their method. Furthermore, the method uses photographic plates which does not allow real time measurements.

The measurement scheme we present in this paper uses a property of the scattered light in the far field limit by illumination of the object with a coherent plane wave. In this case the motion of the pattern is entirely independent of a translation of the scattering object and depends exclusively on its velocity gradient, i.e. on the spatial change of the velocity [7]. It is obvious that with the analysis of the scattered light in the far field limit the information on spatial properties of the scatterer is lost. This means that the measured distortion is an average over the illuminated area. However, we are going to show that with this method the obtained distortions can be determined very accurately, and, in principle, all possible distortion and rotation components can be determined simultaneously.

This method was developed on the basis of a technique to measure velocity gradients in fluid flow. The theory which it is based on is given in [7, 8]. With the experimental set-up presented here the motion of the pattern is determined from the spatial cross-correlation

function of two speckle pictures which are recorded at two successive times. For a known scattering geometry it is then possible to obtain the velocity gradient of the surface motion from the time lag between the two recordings and the translation distance of the speckle pattern.

The method described in this paper will be useful in cases where high accuracy and high spatial resolution is required. It might therefore be interesting for quality control of miniaturized elements. In cases where only one component of the velocity gradient tensor is of interest one can measure the pattern velocity with a diode array detector. This reduces measurement time as well as evaluation time considerably and allows the study of time series of rotations and/or distortions.

2 Theory

Consider a plane light scattering surface (see figure 1). Let us assume that the necessary roughness of the surface can be described as a statistical ensemble of point-like light scattering centres. On illuminating this surface with a plane wave characterized by the wave vector \vec{k}_i a complex scattered light wave results. Any Fourier component of this wave is focussed by use of the lens L_1 on a particular point P on a screen B which coincides with the focal plane of this lens. This secures the pattern on the screen to represent the far field limit of the scattered light.

The amplitude of an arbitrary scattered wave component with wave vector \vec{k}_s on the screen is then given by

$$E_P(\vec{q}, t) = \sum_j E_0(\vec{r}_j) \sigma_j(\vec{q}) e^{-i(\omega t + \vec{r}_j(t) \cdot \vec{q})} \quad (1)$$

In this equation $\sigma_j(\vec{q})$ is the scattering amplitude of the scatterer j , $E_0(\vec{r})$ is the amplitude of the illuminating light wave at the point \vec{r} . The scattering vector \vec{q} is defined by the relation

$$\vec{q} = \vec{k}_i - \vec{k}_s \quad (2)$$

It denotes a definite Fourier component of the scattered light wave.

The surface is now assumed to undergo a distortion with a definite velocity gradient. Then the velocity of the j -th scattering centre is given by

$$\vec{v}(\vec{r}_j) = \vec{v}_o + \hat{\Gamma} \cdot \vec{r}_j \quad (3)$$

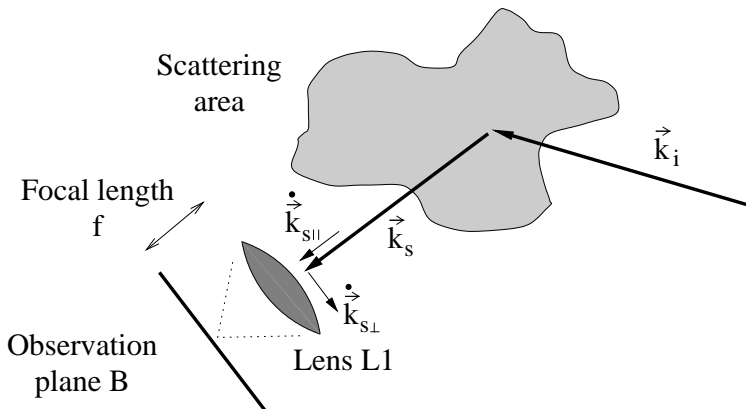


Figure 1: Schematic representation of a light scattering experiment and the observation of the far field intensity pattern.

In this equation \vec{v}_o is the overall velocity of the surface and the tensor $\hat{\Gamma}$ is the velocity gradient tensor with the components

$$\Gamma_{jk} = \frac{\partial v_j}{\partial r_k} \quad (4)$$

The tensor $\hat{\Gamma}$ contains components describing rotation, strain, and shear. The motion of the surface according to equation (3) results in a motion of the speckle pattern. The velocity of

this motion can be described by the temporal change of the vectors of the Fourier components \vec{k}_s of the scattered light wave. According to [7] this is given by:

$$\dot{\vec{k}}_s = \hat{\Gamma}^T \cdot (\vec{k}_i - \vec{k}_s), \quad (5)$$

where the superscript T denotes the transpose of the tensor. Because of the relation

$$|\vec{k}_s| = \frac{2\pi}{\lambda} \quad (6)$$

between the wave vector and the wavelength λ of the used light source Fourier components with wave vectors which do not fulfill this equation should have no experimental significance. Consequently, the wave vectors of all Fourier components which can be observed lie on a sphere in the wave vector space which is known as Ewald sphere (see figure 2).

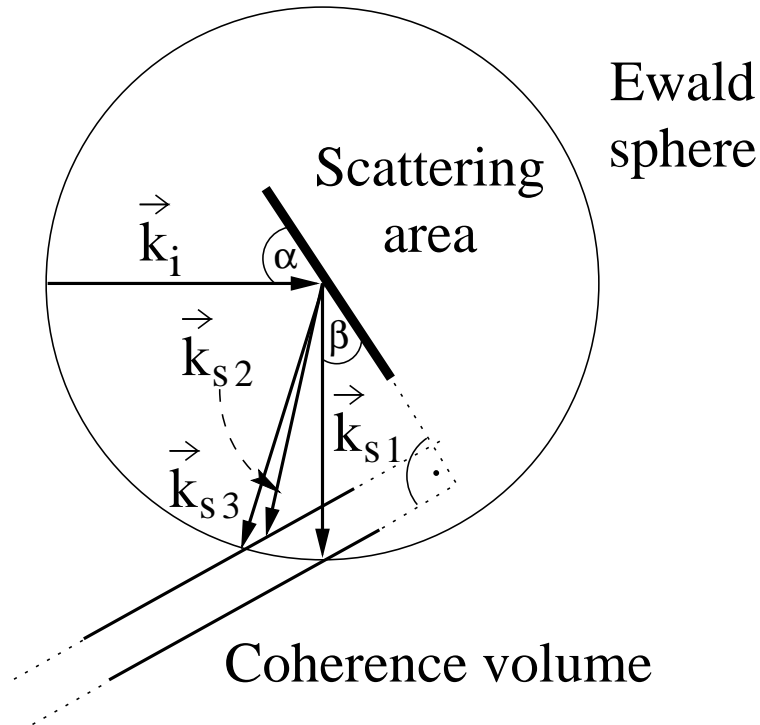


Figure 2: The motion of the wave vector of a scattered light component due to a distortion of a scattering plane surface. Explanation see text.

Therefore, it seems to be obvious that only the components of $\dot{\vec{k}}_s$ perpendicular to \vec{k}_s should be responsible for the speckle motion. For the set-up shown in figure 1 one then obtains with simple geometric considerations the velocity \vec{v}_s of the speckle pattern:

$$\vec{v}_s = f \frac{\dot{\vec{k}}_{s\perp}}{|\vec{k}_s|} \quad (7)$$

However, a more careful analysis of the light scattering shows that one has to take into account possible correlations of different Fourier components of a light wave produced in the way considered here, i.e. by scattering of a coherent light wave in a spatially limited region. For two different Fourier components with wave vectors \vec{k}_{s1} and \vec{k}_{s2} this correlation is proportional to the inverse of the extension of the scattering volume in the direction of

$\vec{k}_{s1} - \vec{k}_{s2}$ [9]. If the vector \vec{k}_{s1} is considered fixed and the vector \vec{k}_{s2} variable one can define a volume enclosed by that surface in the wave vector space where the correlation of the components \vec{k}_{s1} and \vec{k}_{s2} has a fixed value of $1/e$ of its maximum value, which is achieved for $\vec{k}_{s2} = \vec{k}_{s1}$. We call this volume the q-volume of coherence.

The change of the speckle pattern can now be explained in the following way: Consider the centre of the q-volume of coherence fixed to the wave vector which denotes a particular point on the observation screen. Then a motion of this wave vector together with its q-volume of coherence is caused by a distortion of the scattering surface according to equation (5). As long as the q-volume of coherence cuts the Ewald sphere there is a correlation of the two patterns. Only if the q-volume of coherence leaves the Ewald sphere a decorrelation of the pattern appears which is observed as speckle boiling. Consequently, it is then possible to observe speckle motion even if the k-vector of a definite wave component moves away from the Ewald sphere, a motion which we call oblique speckle motion.

A plane scattering surface leads to a q-volume of coherence which is infinite in the direction normal to the plane. This means that regardless of the surface motion there will always be pure speckle motion, and boiling due to a motion of the coherence volume away from the Ewald sphere does not occur (For other sources of boiling see below). This behaviour is illustrated by the well known fact that an arbitrary rotation of an illuminated plane diffraction grating always shows a motion of the diffracted light spots.

The behaviour just discussed is shown schematically in figure 2. Consider a point on the screen which is illuminated by the Fourier component with wave vector \vec{k}_{s1} . Assume that the distortion of the scattering surface is such that this wave vector \vec{k}_{s1} has a certain time later - according to equation (5) - the value \vec{k}_{s2} . Then the second pattern appears as if the wave vector \vec{k}_{s1} had changed to \vec{k}_{s3} .

From these considerations it is now possible to deduce an equation for the observed speckle velocity on the screen on the basis of simple geometric considerations:

$$\vec{v}_s = \frac{f\lambda}{2\pi} \left[\dot{\vec{k}}_s - \frac{\vec{k}_s \cdot \dot{\vec{k}}_s}{\vec{k}_s \cdot \vec{e}} \cdot \vec{e} \right] \quad (8)$$

In this equation \vec{e} is a unit vector normal to the scattering plane pointing towards the illuminated side. It points of course also along the long axis of the q-volume of coherence.

It should be noted that the vector \vec{v}_s of the pattern velocity is a two-dimensional vector in the plane perpendicular to \vec{k}_s , which can easily be verified by multiplying equation (8) by \vec{k}_\perp . Consequently, from a measured pattern velocity only two linear independent components of $\dot{\vec{k}}_s$ can be obtained.

The experiments reported in this paper were performed with set-ups in which the normal of the scattering surface was in the scattering plane, i.e. in the plane defined by the two vectors \vec{k}_i and \vec{k}_s . This choice is by no means necessary but it renders the evaluation of the data rather simple. Two special orthogonal components of the pattern velocity, one in the scattering plane and the other perpendicular to it, can then be expressed in the following way:

$$v_{s\pi} = \frac{\lambda f}{2\pi} \cdot \left(\dot{\vec{k}}_s \cdot \vec{e}_\pi - \frac{\dot{k}_{s||}}{\tan(\beta)} \right) \quad (9)$$

$$v_{s\sigma} = \frac{\lambda f}{2\pi} \cdot \vec{k}_s \cdot \vec{e}_\sigma$$

In this equation $\dot{k}_{s\parallel}$ is the size of that component of \vec{k}_s which is parallel to \vec{k}_s . \vec{e}_π and \vec{e}_σ are orthogonal unit vectors in the observation plane, \vec{e}_σ is perpendicular to the scattering plane and \vec{e}_π is defined by the additional relation $\vec{e} \cdot \vec{e}_\pi = \cos \beta$, where β is the angle between the vector \vec{k}_s and the scattering surface as shown in figure 2.

It should be noted that the diffraction by a plane surface can more easily be treated than using the Ewald construction. However, this more general treatment can easily be extended to scattering of bent surfaces or to not truly two-dimensional ones. In these cases the shape of q-volume of coherence is different from the one we assumed in our measurements.

3 The cross-correlation technique

The velocity \vec{v}_s of the speckle motion can be obtained from two pictures of the speckle pattern recorded with a time lag τ . The patterns seen on the two pictures are shifted with respect to each other. In addition, speckle boiling leads to a random change in the pattern and therefore the pictures are not identical if shifted properly. The most reliable method to calculate the relative shift is to cross-correlate the two pictures and analyse the two-dimensional cross-correlation function.

It is common practice to calculate spatial correlation functions of digital images with the help of the fast Fourier transform algorithm [10, 11]. If $g(\vec{r})$ and $h(\vec{r})$ are two two-dimensional digital images then their cross-correlation function $z(\vec{r})$ is given by

$$z(\vec{r}) = \text{FFT}^{-1}(\text{FFT}(g) \cdot \text{FFT}(h)) \quad (10)$$

The fast Fourier transform algorithm intrinsically assumes a periodic continuation of the pattern which results in a periodicity of the calculated correlation function $z(\vec{r})$. This behaviour restricts the region of the cross-correlation picture, which can be interpreted unambiguously to an area of $N/2 \times M/2$ pixels around the origin.

An example of a correlation function obtained from two successively recorded speckle patterns and calculated in the way described is shown in figure 3.

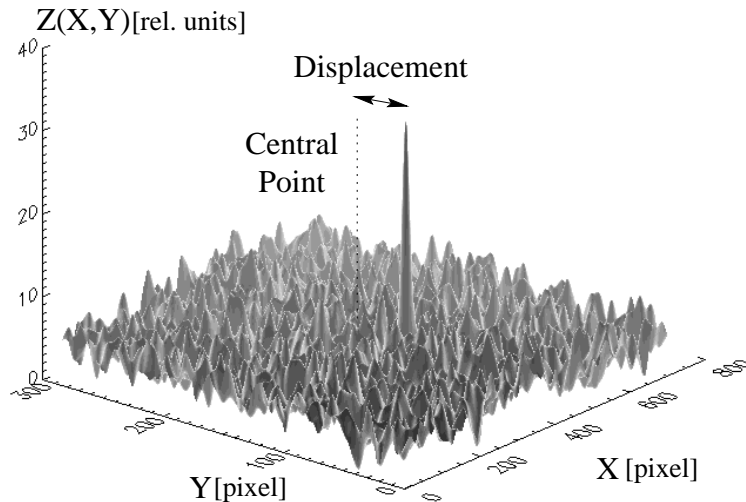


Figure 3: Example of a cross-correlation function, calculated from two intensity patterns successively recorded with a CCD-camera. The shift of the pattern during the time interval between the two recordings is identical to the shift of the maximum in the correlation function relative to the centre point.

Under certain conditions it is possible to determine the position of the maximum with an

accuracy which is much higher than the pixel distance. This can be done if on the one hand the coherence area (speckle size) is significantly larger than the pixel distance, and on the other hand if the form of the ideal correlation function is known. The first condition can easily be met. One has to note, however, that the statistical accuracy of the calculated correlation function decreases with the number of recorded speckles. The second condition is not so strict: Generally, the correlation function is symmetric and the region around the maximum can therefore always be approximated by a general paraboloid.

We fitted the following function with six free parameters to a region around the maximum:

$$F(x, y, \{a_i\}) = a_1 + a_2x + a_3y + a_4xy + a_5x^2 + a_6y^2 \quad (11)$$

by determining the minimum of the quantity

$$\Delta = \sum_{\nu} \sum_{\mu} (F(x_{\nu}, y_{\mu}, \{a_i\}) - z(x_{\nu}, y_{\mu}))^2 \quad (12)$$

where x_{ν}, y_{μ} are the coordinates of the point (ν, μ) in the correlation function. The conditions for a minimum of Δ are $\partial\Delta/\partial a_i = 0$. This leads to a linear system of equations which allows the determination of the a_i and furthermore the calculation of the location (x_m, y_m) of the maximum of $F(x_{\nu}, y_{\mu}, \{a_i\})$. One obtains

$$\begin{aligned} x_m &= \frac{2a_2a_6 - a_3a_4}{a_4^2 - 4a_5a_6} \\ y_m &= \frac{2a_3a_5 - a_2a_4}{a_4^2 - 4a_5a_6} \end{aligned} \quad (13)$$

Due to the calculation of the correlation function from a finite set of pixels the result is far from ideal. Consequently, besides the ‘true’ maximum (the one which results from the pattern motion) in the correlation function further ‘random’ maxima occur. In addition, speckle boiling decreases the numerical value of the ‘true’ maximum of the correlation function. In this way it may happen that the numerical values of the random maxima are of about the same size as that of the true one. In such cases the correlation function cannot be interpreted unambiguously. It is therefore necessary to introduce a criterion which allows to assess the validity of the main maximum. We used two quantities for this validity check:

- The ratio of the heights of two most prominent maxima

$$SNR_{pp} = \frac{z_{\text{main maximum}}}{z_{\text{second maximum}}} \quad (14)$$

- The ratio of the height of the highest maximum and the root of the variance of the background

$$SNR_{pr} = \frac{z_{\text{main maximum}}}{e_{rms}} \quad (15)$$

with $e_{rms} = \sqrt{\frac{1}{NM} \sum_{\nu=-\frac{N}{2}}^{\frac{N}{2}} \sum_{\mu=-\frac{M}{2}}^{\frac{M}{2}} (z(x_{\nu}, y_{\mu}) - \bar{z})^2}$

We used the quantity SNR_{pp} for the check of the validity of a measurement because it turned out to be well suited for that purpose and it can be calculated very fast. The criterion we used is

$$SNR_{pp} > 1.5 \quad (16)$$

Only about 1 % of all measurements did not fulfill this criterion and were discarded.

4 Experiments

The general set-up which was used for our experiments is shown schematically in figure 4.

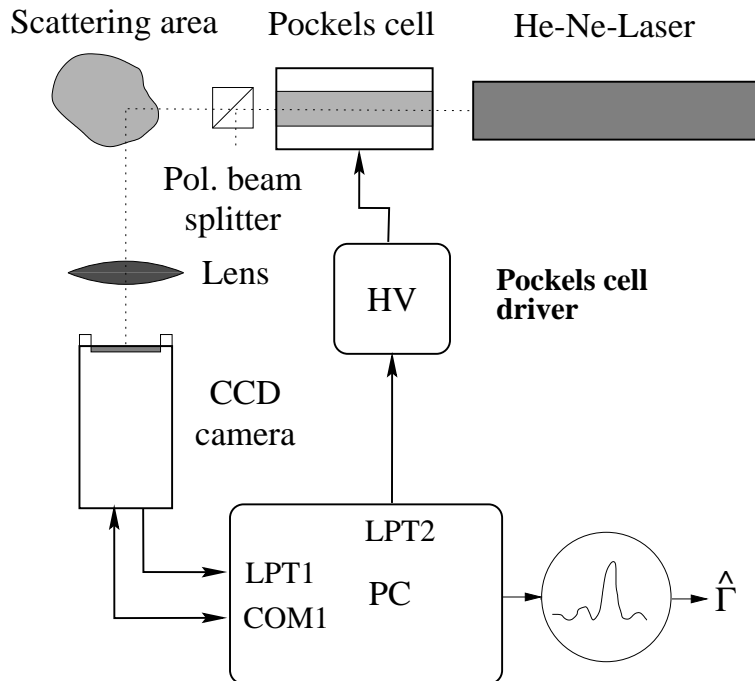


Figure 4: General set-up for the measurement of velocity gradients of a scattering surface by use of a CCD-camera.

A 5 mW HeNe-laser is used as coherent light source. A Pockels cell between two polarizers served as a fast optical shutter to control the illumination of the samples. The high voltage for the Pockels cell is supplied by a power supply which is controlled by a PC. In this way it was possible to achieve switching times for the laser light reproducible on a microsecond scale. The PC also controls the CCD-camera.

The pulsed laser beam reaches the plane surface under examination under an angle α , the scattered light is observed under an angle β with respect to the surface. To make sure that the scattered light is observed in the far field limit we placed a lens between scattering surface and camera in such a way that the sensitive area of the camera coincides with the focal plane of the lens.

The special CCD-camera (PCO Double Flash) allows the recording of two pictures with a definite time interval which can be chosen between 300 ns and 40 ms. For the double recordings the camera works in an interlaced mode with 754×286 pixels for each picture. External triggers supplied from the PC control the recording of the camera.

The method we describe here was applied to three different distortions/rotations with velocity gradients which were also determined by independent means. We present here the results of measurements of rotation (figures 6,7,8), strain (figures 10, 11, 12), and bend (figure 13).

4.1 Rotation

For these measurements a rotating disc was used. It was set in motion by an electric motor to which it was connected by a rubber belt. The axis of rotation was positioned in a horizontal plane (in our notation the x-y plane). A sketch of this scattering geometry is given in figure 5. From equation 3 follows that the speckle motion in this case is perpendicular to the scattering plane. It is thus possible to measure the gradient component $\frac{\partial v_x}{\partial y}$.

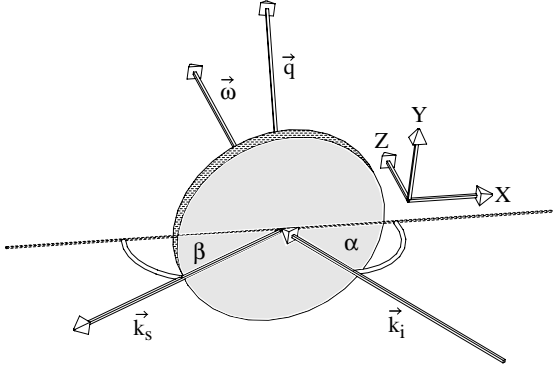


Figure 5: The scattering geometry for the rotation measurements and the definition of the angles α and β

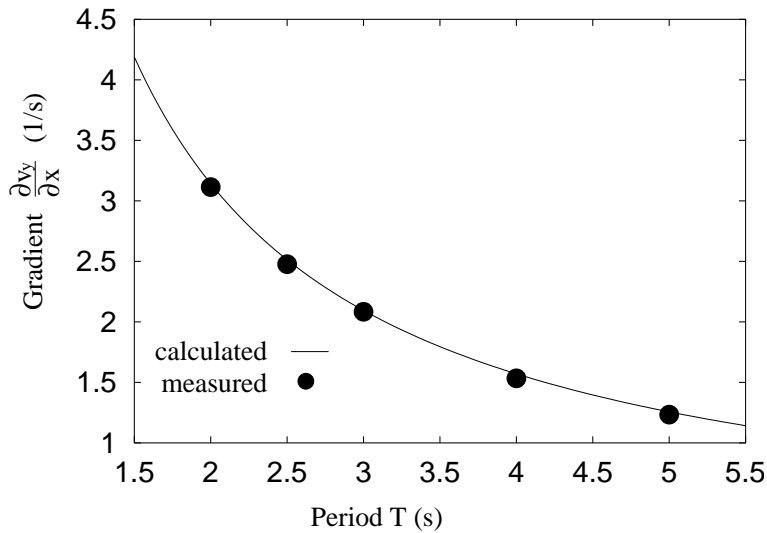


Figure 6: Comparison of measured and calculated gradient component $\frac{\partial v_y}{\partial x}$ as a function of the period of the rotating scattering surface. The scattering angle β was kept fixed at 30° .

Equation 9 leads to a very simple connection between this gradient component and the

measured speckle velocity v_{sy} :

$$\frac{\partial v_x}{\partial y} = \frac{v_{sy}}{f(\cos \alpha - \cos \beta)} \quad (17)$$

We choose in our experiments rectangle scattering, i.e. $\alpha + \beta = 90^\circ$

Figure 6 shows results of measurements of the gradient component $\frac{\partial v_y}{\partial x}$ as a function of the period of revolution of the rotating disc. This period was determined by use of an opto-coupled interrupter module. The angle β was 30° and consequently $\alpha = 60^\circ$ with an accuracy of $\pm 1^\circ$. We furthermore measured the dependence of the velocity of the speckle pattern on the angle β , results are shown in the upper part of figure 7.

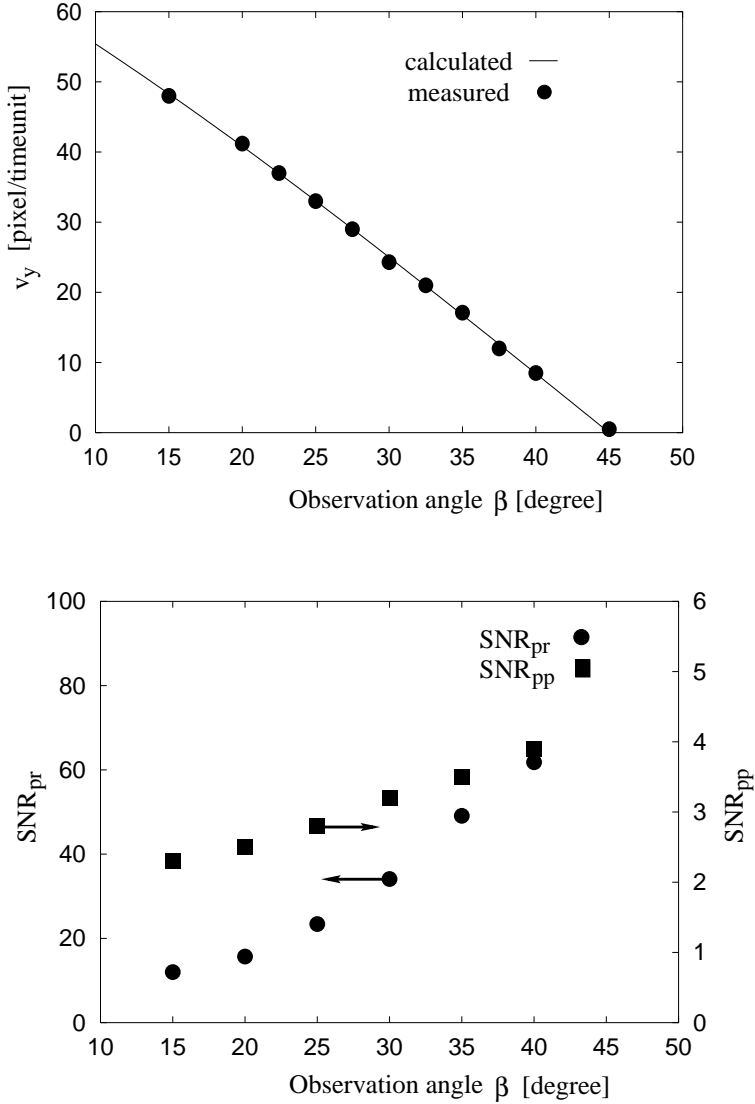


Figure 7: Upper part: Measured speckle velocity v_y^s as a function of the scattering geometry with $\alpha = 90^\circ - \beta$ Lower part: The signal-to-noise ratio of the calculated velocities obtained from 10 measurements for each data point.

The scatter in the determined gradient values is - except for very small β - less than 1%,

which means that reliable gradient values can be obtained from one single measurement consisting just of one double exposure.

The quality of the determined gradient data can be assessed with the parameters R_{pp} and R_{pr} introduced in the last section. The lower part of figure 7 shows results obtained from measurements using paper as a scattering medium, again as a function of β .

The lower limit for the detection of a rotation using our method depends mainly on the illuminated area: Let us consider a fixed velocity gradient which results in a fixed speckle velocity. It is obvious, that the accuracy of the determination of the speckle velocity decreases inversely proportional to the speckle size. Now, the speckle size just varies inversely proportional to the diameter of the scattering area. Therefore, the accuracy of the determined gradient data increases proportional to the size of the scattering area. It is tacitly assumed in this reasoning that the laser power is sufficient for photon statistics to be negligible and that furthermore the optical set-up is optimized in such a way that the ratio of speckle size to pixel distance is kept constant.

For our set-up with a diameter of the illuminated area of about 0.7mm and a detectable speckle motion of 0.1 pixel distance (see section discussion) we can resolve a rotation angle of 0.001° .

An increase of the distance between the rotation axis and the area of illumination leaves the velocity gradient constant whereas the velocity of the scattering area increases. It is then possible to study two different aspects of the obtained gradient values:

- Are the experimentally determined gradient values really independent of the linear velocity of the scattering object?
- Does the boiling of the speckle pattern increase the data scatter significantly?

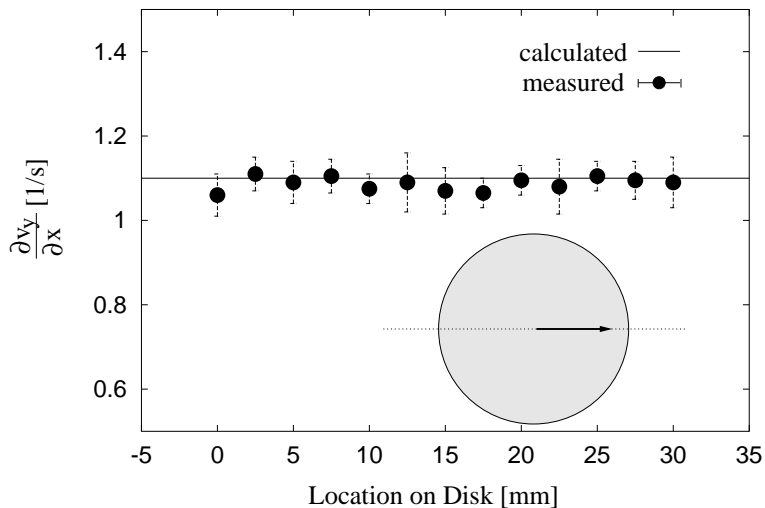


Figure 8: The measured gradient component $\frac{\partial v_y}{\partial x}$ as a function of the distance of the scattering area from the rotation axis.

These two questions can be answered with help of figure 8. On the one hand no systematic deviation of the gradient values can be observed. On the other hand there is also **no** increase of the scatter for larger velocities of the scattering area. The small amount of scatter shown in the figure is mainly due to slight variations of the angular velocity of the rotating disc.

4.2 Strain

The strain measurements were performed with a flat rubber tape ($6 \times 70 \times 1\text{mm}^3$). One of its ends was fixed, the other was attached to the membrane of a loud-speaker. A saw tooth voltage controlled by a PC was applied to the loud-speaker which led to a strain of the rubber nearly linear in time between the jumps. The set-up is shown schematically in figure 9. The absolute amount of strain of the rubber tape was determined by measuring

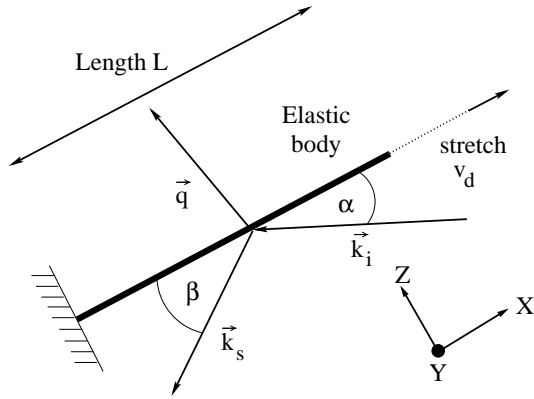


Figure 9: The scattering geometry for the strain measurements.

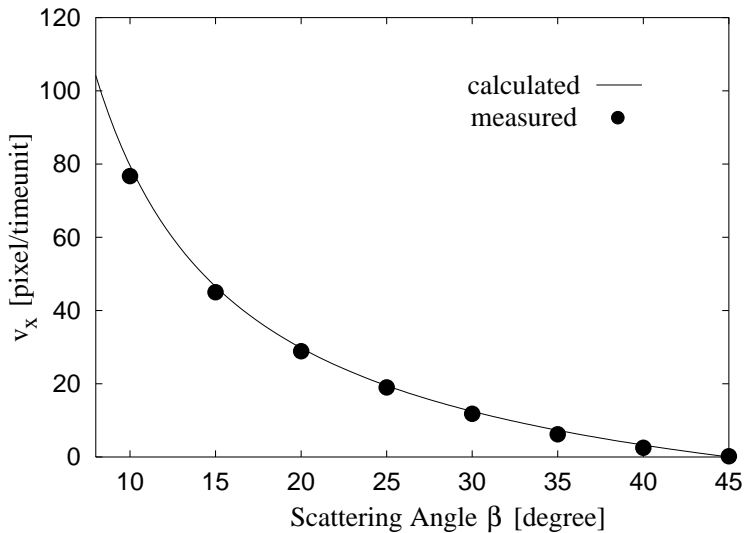


Figure 10: The speckle velocity caused by stretching the scattering surface as a function of the scattering angle β . The straight line is calculated from the velocity $v_d = 3.9 \frac{\text{mm}}{\text{s}}$ of the end of the tape.

the maximum displacement of the membrane of the loud-speaker with a micrometer screw and assuming a constant force constant of the rubber.

The motion of the rubber tape was restricted to the scattering plane (the x-y-plane) which results in a speckle motion in this plane too. The speckle motion is then exclusively determined by the gradient component $\frac{\partial v_x}{\partial x}$. It is not difficult to deduce from equation (9) the

connection between speckle velocity and velocity gradient for this case:

$$\frac{\partial v_x}{\partial x} = \frac{v_{sx} \sin \beta}{f(\cos \alpha - \cos \beta)} \quad (18)$$

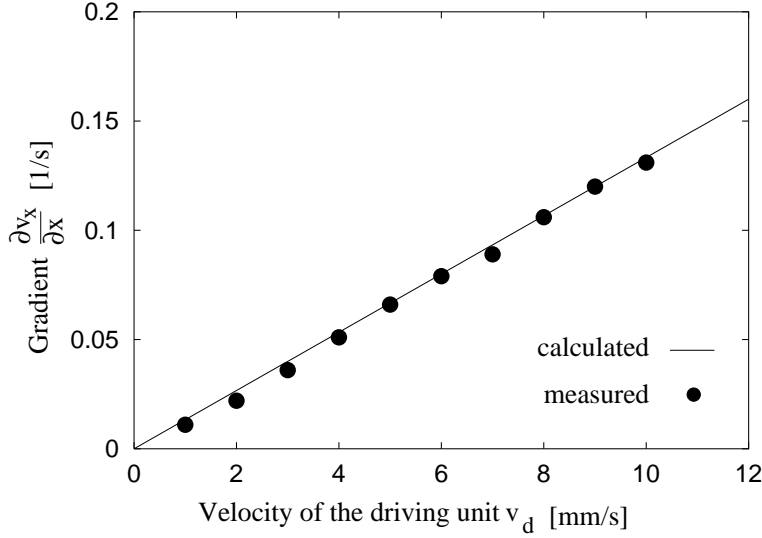


Figure 11: Comparison of the measured gradient component $\frac{\partial v_x}{\partial x}$ and the one calculated from the velocity v_d of the end of the rubber tape. The scattering angles are $\alpha = 30^\circ$ and $\beta = 90^\circ$.

Figure 10 shows the results of measurements of the speckle velocity v_{sx} as a function of the angle β with $\alpha + \beta = 90^\circ$. In this case we have speckle motion which we call oblique, because the motion in q-space is not tangential to the Ewald sphere (c.f. section 2). The straight line in this figure represents the speckle velocity calculated from the velocity v_d of the moving end of the rubber tape, which was in this case 3.9mm/s. For $\beta = 90^\circ$ the influence of $\vec{k}_{a\parallel}$ vanishes and the speckle motion in q-space is tangential to the Ewald sphere. This leads to an even simpler relation than the last one:

$$\frac{\partial v_x}{\partial x} = \frac{v_{as}}{f \cos \alpha} \quad (19)$$

The dependence of $\frac{\partial v_x}{\partial x}$ on the velocity v_d of the loud-speaker membrane is shown in figure 11. The straight line represents the connection obtained from the focal length of the lens and the angle α .

Figure 12 shows the dependence of the speckle velocity on the angle α with β kept fixed at 90° . Again, the experimental data follow closely the theoretical ones.

The lower limit for a detectable strain with the set-up we used and with a scattering geometry determined by $\alpha = 80^\circ$ and $\beta = 10^\circ$ was $\frac{dL}{L} = 2 \cdot 10^{-5}$, where we again assumed a minimum detectable speckle motion of 0.1 pixel distance.

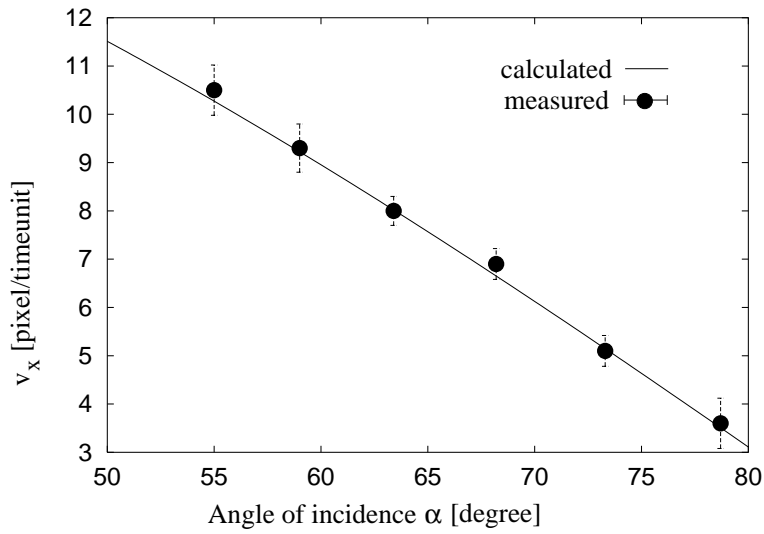


Figure 12: The speckle velocity as a function of the angle of incidence α . The angle β was kept fixed at 90° .

4.3 Bend

For these measurements a flat plastic rod was used. Again, one end was mounted to a fixed support, the other was attached to the membrane of the loud-speaker rectangular to the motion direction of the membrane. The bend of the rod was restricted to the scattering plane. The scattering geometry was essentially identical to the one shown in figure 9, the only difference being a controlled motion of the free end of the elastic body perpendicular to its long axis, i.e. in z -direction. Due to the small extension of the end the rod of about 1 mm compared to its length of 750 mm it is admissible to apply the theoretical results of the bending of an elastic rod. The transverse motion amplitude of the neutral line of the rod is then given by

$$w(x) = \frac{3D}{L^3} \left(\frac{Lx^2}{2} - \frac{x^3}{6} \right) \quad (20)$$

Here x is the coordinate along the long axis of the rod and D the shift of the end of the rod. The largest curvature which follows with the given parameters from this equation has a radius of about 1 m. With a thickness of the rod of 1 mm one can safely neglect the distortion of its surface. Speckle motion is then caused by a local rotation of the surface around a vertical axis, and the only non-vanishing elements of the gradient tensors are

$$\frac{\partial v_z}{\partial x} = -\frac{\partial v_x}{\partial z} = \frac{3v_D}{L^3} \left(Lx - \frac{x^2}{2} \right) \quad (21)$$

where v_D is the velocity of the moving end of the rod. The application of equation (9) leads for the considered case to the following connection between the measured speckle velocity and the gradient component:

$$\frac{\partial v_z}{\partial x} = \frac{v_{sx} \sin \beta}{f(1 - \sin(2\beta + \alpha))} \quad (22)$$

Since according to equation (21) the bend of the rod varies along the long axis we measured

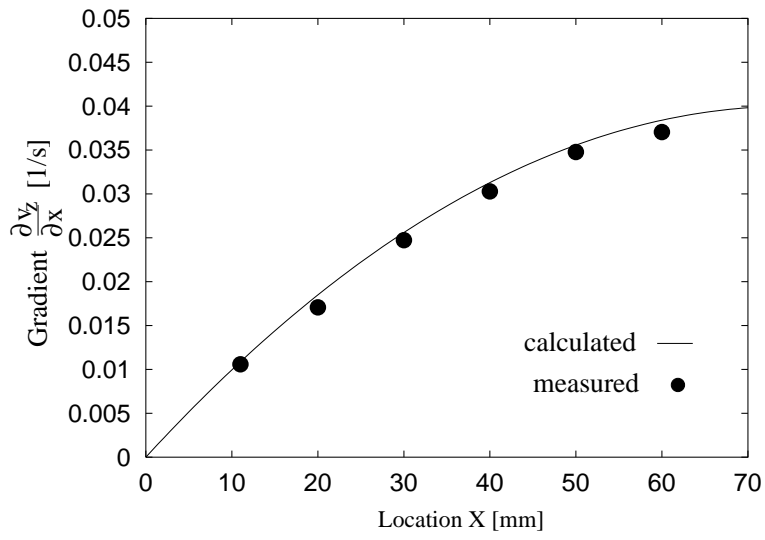


Figure 13: The gradient component $\frac{\partial v_z}{\partial x}$ as a function of the location on the bent rod.

the gradient component $\frac{\partial v_z}{\partial x}$ along this axis. The result of these measurement are shown in figure 13.

For the bend measurements we performed no analysis of the scatter in the obtained gradient values because such an analysis would be based on approximations which renders it somewhat dubious.

5 Discussion

The gradient tensor of a plane consists of six independent components, They describe three rotations around orthogonal axes, two orthogonal shearing distortions within the plane and a uniform strain. It is generally possible to measure all of these components with the method we presented. Of course, a simultaneous measurement requires an experimental set-up which allows to record three speckle patterns in different directions.

In order to demonstrate the general suitability of the method we performed measurements on surfaces which underwent rather simple distortions or rotations. We could demonstrate that the method can be used to measure very small distortions/rotations and that the measured gradient values are very reliable. It represents no problem to obtain rather high spatial resolution, we used in our measurements illuminated areas with diameters down to 0.7 mm.

For a successful application of the described method the two following aspects have to be considered:

- In the experiments described here the influence of speckle boiling could be neglected. This was due to the following fact: The linear motion of the scattering area was in all cases so small that the light for the two recordings resulted from almost identical parts of the surface. In case of large linear velocity and small gradients the situation will be unfavourable: Either one takes the two recordings with a small time delay which results in a small relative shift of the two patterns, or - for a larger delay - the correlation of the two patterns will be small. If we call the in-plane motion velocity v_s and the diameter of the illuminated area parallel to the direction of this velocity d_s we obtain the following condition for the maximum time delay:

$$\tau < \frac{d_s}{v_s} \quad (23)$$

- A very severe source of speckle boiling represents multiple scattering in the scattering surface. For instance, measurements with a non-absorbing opaque plastic bar as scattering medium were not successful because of the very small correlation of the two speckle patterns even for very small time delays.

From series of measurements where all parameters were kept constant we deduced that the scatter of a single measurement of the pattern motion to 0.07 pixel distances. This is slightly less than the value of 0.1 pixel we used to assess the sensitivity of our method.

In order to obtain good results one has to consider two further parameters. This is on the one hand the ratio of the speckle size to the pixel size. For the fit procedure we performed this ratio should be at least 6. On the other hand, there should be a minimum number of recorded speckles, otherwise the scatter in the calculated correlation functions becomes very large and the main maximum cannot safely be discriminated from random ones. We found that the number of speckles in the direction of the pattern motion should not be less than about 40. This is in accordance with the findings of Kriegs et al. [8].

6 Acknowledgement

We are indebted to Dr. B. Schwark-Werwach who initiated this research and supported it technically in its first stages. We furthermore thank H.Rohbeck for his technical assistance.

References

- [1] W.C. Wang, C.H. Hwang, S.Y. Lin, Vibration measurement by time-averaged electronic speckle pattern interferometry methods, *Applied Optics* (1996), **35**, 4502-4509
- [2] W.Z.L. Zhuang, J.P. Baird, H.M. Williamson, R.K. Clark, Three-dimensional displacement measurement by a holospeckle interferometry method, *Applied Optics* (1993), **32**, 4728-4737
- [3] E. Archbold, J.M. Burch, A.E. Ennos, Recording of In-Plane Surface Displacement by Double-Exposure Speckle Photography, *Opt. Acta* (1970), **17**, 883-895
- [4] A. Hayashi, Y. Kitagawa, High-resolution rotation-angle measurement of a cylinder using speckle displacement detection, *Applied Optics* (1983), **22**, 3520-3519
- [5] N.Takai, T. Asakura, Vectorial measurement of speckle displacement by 2-D electronic correlation method, *Applied Optics* (1985), **24**, 660-665
- [6] W. Z. L. Zhuang, J. P. Baird, H. M. Williamson, and R. K. Clark, Three-dimensional displacement measurement by a holospeckle interferometry method, *Applied Optics* (1993) **32**, 4728-4737
- [7] C. Keveloh, W. Staude, The measurement of velocity gradients in laminar and turbulent flow, *J. Phys. D:Appl. Phys.* (1988), **21**, 237-245
- [8] Krieger, H. and Staude, W. , A laser pulse technique for the measurement of time-resolved velocity gradients in fluid flow, *Meas. Sci. Technol.* (1995) **6** . 653-662
- [9] A.Clark, J.H.Lunacek and G.B.Benedek, "A study of Brownian motion using light scattering", *Am. Journal Phys.* (1970) **38** 575-585
- [10] R.C. Gonzalez, P. Wintz, *Digital Image Processing*, Addison Wesley, 1977
- [11] E. Oran Brigham, *The fast Fourier transform*, 1974, 8th edition, Prentice-Hall